# Streamtube Expansion Effects on the Darrieus Wind Turbine

Ion Paraschivoiu*
*Ecole Polytechnique de Montréal, Montréal, Canada*
and
Philippe Fraunié† and Claude Béguier†
*Institut de Mécanique Statistique de la Turbulence, Marseilles, France*

**The purpose of the work described in this paper was to determine the aerodynamic loads and performance of a Darrieus wind turbine by including the expansion effects of the streamtubes through the rotor. The double-multiple streamtube model with variable interference factors was used to estimate the induced velocities with a modified CARDAAV computer code. Comparison with measured data and predictions shows that the streamtube expansion effects are relatively significant at high tip-speed ratios, allowing a more realistic modeling of the upwind/downwind flowfield asymmetries inherent in the Darrieus rotor.**

## Two-Actuator-Disk Models

THE Darrieus rotor is modeled by a pair of actuator disks arranged in tandem and capable of accounting for the difference in flowfield between the upwind and downwind half-cycles of the turbine. This concept, initially proposed by Lapin,[1] gave rise to the development of a large number of aerodynamic models for studying the Darrieus wind turbine. The major differences between the various models are due to the assumptions used and the means of calculating the induced velocities through the rotor. However, several authors incorporated Holme's remark regarding the vortex theory[2] in their momentum theories: that half the velocity retardation along a streamline occurs within the rotor.

Thus, using linear aerodynamics and ignoring the effects of drag and stall, Sharpe and Read[3] found a simple expression for the interference factors needed to calculate the induced velocities. The flowfield through the turbine was supposed to consist of straight but not parallel streamlines, yet the velocities everywhere were parallel to the $V_\infty$ direction. A theoretical optimization technique was subsequently developed by Loth and McCoy[4] for straight-bladed Darrieus wind turbines. They considered two semicylindrical actuator disks in series with separate cosine-type interference factors for the upwind and downwind half of the rotor; with this velocity distribution, the rotor blades become unloaded near the junction of the two rotor halves. In their inviscid analysis, the same authors used disks of equal area and found a Betz-type limit higher than the conventional value. An analysis for two uniformly loaded actuator-disks given by Newman[5] showed that the standard predictions ($C_{pmax} = 16/27$) are pessimistic and he calculated a new value of $C_{pmax} = 16/25$, which corresponds to those estimated by Ref. 4.

A more practical analytical model was developed by Paraschivoiu[6] using two constant interference factors over the front and back halves of the rotor for estimating the induced velocities. This double-multiple streamtube model is useful for predicting the overall aerodynamic performance and loads and for structural dynamic studies of the Darrieus straight- and curved-bladed rotor. These different characteristics were determined using an inexpensive CARDAA computer code capable of distinguishing between upwind and downwind blade forces. Performance/load calculations were made on the basis of the local Reynolds number and the local angle of attack.

Using a method similar to Strickland's multiple streamtube theory,[7] Templin[8] treated the upwind and downwind faces of the rotor separately and derived a model that furnishes the asymmetric airfoil characteristics. At Sandia Laboratories, Berg[9] considered a sine distribution for the induced velocities through the rotor, which was later incorporated in the double-multiple streamtube model.[6] The SIDIF computer code used in this case includes nonconstant interference factors, which conserve mass by allowing the stream tubes to spread. However, since the SIDIF model breaks down at high tip-speed ratios, work is now under way on a so-called "independent double-multiple streamtube" model with the INDOMS computer code, where the streamtubes in the upwind and downwind halves of the rotor are supposed independent of each other; the expansion of the streamtube is confined to the horizontal plane and the equilibrium- plane velocity is assumed nonuniform.

The Darrieus wind turbine was also studied by Comolet et al.[10] using a bidimensional multiple streamtube model that takes account of both the widening and the lateral displacement of the streamtubes. However, the performance calculations were made on the basis of a single Reynolds number, whereas in reality the operation of the Darrieus turbines is such that the Reynolds number varies cyclically as a function of the blade position and, furthermore, for the curved-bladed rotor *Re* also varies along the blade span.

According to the two-actuator disk theory the previous double-multiple streamtube model[6] was improved by considering the variation in the upwind and downwind induced velocities as a function of the azimuthal angle for each streamtube.[11] Among the many two-actuator disk models, only the latter includes the influence of all secondary effects, namely the blade geometry and profile type, the rotating tower, and the presence of struts and aerodynamic spoilers on the Darrieus turbine.[12]

For this work, the double-multiple streamtube model with variable interference factors based on a modified CARDAAV computer code, the CARDAAX, was used for the calculations.

Received Aug. 10, 1984; revision received Oct. 8, 1984. 

*Associate Professor, Department of Mechanical Engineering and Consultant at Institut de Recherche d'Hydro-Québec. Member AIAA.

†Senior Scientist, Department of Mechanical Engineering.

## Streamtube Expansion Model

The Darrieus machine is a complex aerodynamically unsteady configuration: during one revolution alone, significant periodic variations occur in the flow direction, relative velocity, and angle of attack. Furthermore, the airflow is cut twice by the blades during one cycle, with the result that the downwind half-cycle of the rotor is strongly disturbed by the upwind half-cycle.

Within each horizontal slice (or streamtube), the flow diverges toward the downwind sector because the velocity decreases, causing the streamtube to expand. Thus, in a realistic model, the upwind disk area must be less (and the downwind disk area greater) than half the blade swept area. A large portion of the upwind velocity is lost and the velocity entering the downwind half of the rotor is highly distorted.

A simplified physical model of the flowfield in a horizontal slice of the rotor, which conserves mass by allowing the expansion of the streamtubes, is presented in Fig. 1. The streamlines $J$ and $J+1$ within the rotor are not parallel, with the result that the width of each streamtube varies continuously along its entire length. The simple physical model used here is not too unrealistic compared with Holme's vortex theory[2] and Comolet's flow visualization.[10]

For a horizontal slice of unit height at a level $Z$ of the rotor, $d\ell_\infty$, $d\ell$, $d\ell_e$ represent the incremental width of the streamtube cross sections in the undisturbed and upwind zones and on the equilibrium plane, respectively. The induced velocities $V$ and $V_e$ were considered parallel to the undisturbed wind velocity $V_{\infty i}$. Assuming ambient pressure in all sections of the upwind half of the rotor ($-\pi/2 \le \theta \le \pi/2$) and applying Bernoulli's equation,

$$\rho V_{\infty i} d\ell_\infty = \rho V d\ell = \rho V_e d\ell_e \tag{1}$$

Using the definition of the upwind interference factor $u(\theta)$

$$V = \tfrac{1}{2}(V_{\infty i} + V_e) = u V_{\infty i} \tag{2}$$

in Eq. (1), we obtain

$$V_{\infty i} d\ell_\infty = V_{\infty i} u d\ell = (2u-1) V_{\infty i} d\ell_e \tag{3}$$

Since $\ell = r\sin\theta$, Eq. (3) becomes

$$d\ell_\infty = ru\cos\theta d\theta = (2u-1) d\ell_e \tag{4}$$

The expanding lateral displacement of the streamline can be determined with respect to an undistorted central streamline, XOX', which corresponds to an azimuthal angle $\theta = 0$ deg. Thus, on the upwind half of the rotor, with a local radius $r$, the flowfield is defined by the streamline coordinates as functions of the azimuthal angle and the upwind interference factor,

$$\ell_\infty = \int_0^\theta ru\cos\theta d\theta \tag{5a}$$

$$\ell = \int_0^\theta ru\cos\theta d\theta \tag{5b}$$

$$\ell_e = \int_0^\theta r\left(\frac{u}{2u-1}\right)\cos\theta d\theta \tag{5c}$$

These expressions allow each streamline in the three sections on the upwind half of the rotor to be plotted. It is now possible to calculate the width of the cross-sectional area of the streamtube by integrating Eqs. (5a) and (5c) between $-\pi/2$ and $\pi/2$,

$$L_\infty = \int_{-\pi/2}^{\pi/2} ru\cos\theta d\theta \text{ in the undisturbed region}$$

$$L = \int_{-\pi/2}^{\pi/2} r\left(\frac{u}{2u-1}\right)\cos\theta d\theta \text{ in the upwind zone of the rotor}$$

The upwind intereference factor $u(\theta)$ varies from one streamline to another and, in order to solve the downwind flowfield spectrum, the upwind sector characteristics must be calculated first.

The $u(\theta)$ values can be calculated by either an iterative or an approximative technique. A reasonable approximation allows us to pass in successive steps from a known streamline $J$ to a neighboring unknown streamline $J+1$, assuming that $J$ is defined by its coordinates with respect to the central streamlines $\ell_{\infty j}, \ell_j, \ell_{ej}, \ell'_j$, and $\ell''_j$ and the velocities $V_{\infty j}$, $V_j$, $V_{ej}$, $V'_j$, and $V''_j$. The following interference factors are also known:

$$u_j = V_j / V_\infty \text{ and } u'_j = V'_j / [(2u-1) V_\infty]$$

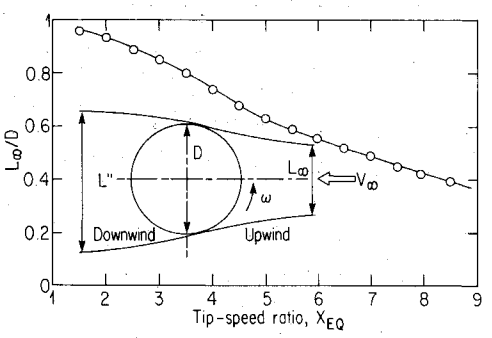


**Fig. 2 Reduction of the streamtube in the undisturbed part of the rotor vs the tip-speed ratio.**

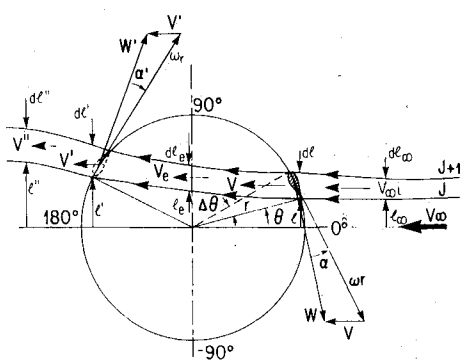


**Fig. 1 Simplified physical model of the flowfield in a horizontal slice of the rotor.**

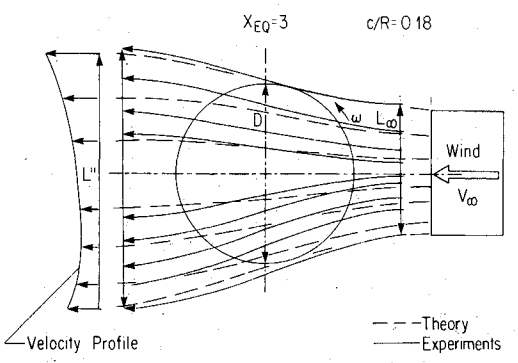


**Fig. 3 Curve streamlines through the rotor, calculation and experiments.**

The continuity equation applied to $J+1$ gives

$$V_{\infty i}\mathrm{d}\ell_\infty = V_j\mathrm{d}\ell_j = V_{ej}\mathrm{d}\ell_{ej} = V_j'\,\mathrm{d}\ell' = V_j''\,\mathrm{d}\ell'' \tag{6}$$

With the expressions

$$V_j = u_j V_{\infty i} \tag{7}$$

$$V_{ej} = (2u_j - 1)\,V_{\infty i} \tag{8}$$

$$V_j' = (2u_j - 1)\,u_j'\,V_{\infty i} \tag{9}$$

$$V_j'' = (2u_j - 1)\;(2u_j' - 1)\,V_{\infty i} \tag{10}$$

Eq. (6) becomes

$$\mathrm{d}\ell_\infty = u_j\mathrm{d}\ell = (2u_j - 1)\,\mathrm{d}\ell_e = (2u_j - 1)\,u_j'\,\mathrm{d}\ell'$$

$$= (2u_j - 1)\,(2u_j' - 1)\,\mathrm{d}\ell'' \tag{11}$$

and it was found that

$$\mathrm{d}\ell_\infty = u_j\mathrm{d}\ell \tag{12}$$

$$\mathrm{d}\ell_e = [u_j/(2u_j - 1)]\,\mathrm{d}\ell \tag{13}$$

$$d\ell' = u_j/[(2u_j - 1)\,u_j']\,\mathrm{d}\ell \tag{14}$$

$$\mathrm{d}\ell'' = u_j/[(2u_j - 1)\,(2u_j' - 1)]\,\mathrm{d}\ell \tag{15}$$

For an arbitrarily small value of $\mathrm{d}\ell = r\cos\theta\mathrm{d}\theta$ defining $J+1$, it is possible to calculate $\mathrm{d}\ell_\infty$, $\mathrm{d}\ell_e$, $\mathrm{d}\ell'$, and $\mathrm{d}\ell''$ and, then, to estimate the coordinates $\ell_{\infty,j+1}$, $\ell_{j+1}$, $\ell_{e,j+1}$, and $\ell_{j+1}'$.

For this new streamline a new azimuthal angle is found, $\theta_{j+1} = \theta_j + \mathrm{d}\theta$, from which new values can be calculated successively for $u_{j+1}$ and $u_{j+1}'$ and, consequently, the velocities $V_{j+1}$, $V_{e,j+1}$, $V_{j+1}'$, and $V_{j+1}''$. Similarly, if the characteristics of $J+1$ are known, the next streamline can be calculated until the entire flowfield through the rotor is built. The input streamtube cross-section $L_\infty$ is calculated by integrating $\mathrm{d}\ell_\infty$, while the output streamtube cross section $L''$ is given by integration of $\mathrm{d}\ell''$.

The practical model considers an integral formulation in a horizontal slice of unit height for which the continuity equation becomes

$$V_\infty L_\infty = VL = V_e L_e = V'L' = V''L'' \tag{16}$$

On the other hand, the speed ratios $u = V_e/V_\infty$ calculated for $L'$ in the downstream part are known. From these it may be deduced that

$$L'/L = V/V' \tag{17}$$

Meanwhile, Glauert's relations

$$(V_\infty - V)/V_\infty = (V - V_e)/V \tag{18a}$$

$$(V_e - V')/V_e - (V' - V'')/V' \tag{18b}$$

yield

$$\frac{L'}{L} = \frac{1+u}{u(1+u')} \tag{19}$$

At a given width, $L'$ corresponds to a value of the interference factor $u'$, calculated interactively, from which a new value of $L'$ can be deduced up to convergence. The known value of $L'$ can then be used to determine the limits of the downwind streamtube $\theta_1'$ and $\theta_2'$

$$\theta_2' = |\arcsin(|\sin\theta_1'| + L'/r)| \tag{20}$$

On the basis of the foregoing development, an attempt was then made to introduce the simplest possible modifications into the CARDAAV program.[13] These modifications affect the calculations related to the downwind part of the rotor and involve an additional iterative process over the entire width $L'$ of the downwind streamtube. It is important to respect the undistorted central line separating the upwind part into two halves; the latter will in fact be studied starting from the central line (see Fig. 2). The major difficulty is to identify the tubes, since the direction of the calculation is sometimes inverted and the calculation points in the tubes depend on the width of the latter. Each downwind tube is associated with the corresponding upwind tube by incrementing the tube number. The last downwind external stream tube is defined with respect to the rotor ($\theta_2' = \pi/2$ or $3\pi/2$) and is associated with a corresponding part of the upwind tube. Some upwind streamtubes may not cross the downwind part. Furthermore, the calculation does not allow some part of the upwind zone downwind of other parts in the same zone since the velocities are considered unidirectional. The calculation called for a modification to the aerodynamic-load subroutine by changing the momentum equation, mainly because of the grid used.

Application of the blade element theory and the momentum equation for each streamtube gives a transcendental equation for the upwind interference factor $u(\theta)$, which was demonstrated in Ref. 11,

$$u(\theta) = KK_o\eta \Big/ \left[KK_o\eta + \int_{\theta-\Delta\theta/2}^{\theta+\Delta\theta/2} f(\theta)\,\mathrm{d}\theta\right] \tag{21}$$

where $K$ is a geometrical parameter of the rotor $K = 8\pi r/Nc$, $K_o$, is a function of $\theta$, $K_o = \sin(\theta + \Delta\theta/2) - \sin(\theta - \Delta\theta/2)$, and $\eta = r/R$.

$$f(\theta) = \left(\frac{W}{V}\right)^2 \left(C_N\cos\theta + C_T\frac{\sin\theta}{\cos\delta}\right) \tag{22}$$

$$C_N = C_L\cos\alpha + C_D\sin\alpha \tag{23}$$

$$C_T = C_L\sin\alpha - C_D\cos\alpha \tag{24}$$

The airfoil lift and drag coefficients, $C_L$ and $C_D$ respectively, are obtained by interpolating test data using both the local Reynolds number and the angle of attack.

Similarly, we can calculate the downwind interference factor $u'(\theta)$,

$$u'(\theta) = -KK_o\eta \Big/ \left[KK_o\eta + \int_{\theta-\Delta\theta/2}^{\theta+\Delta\theta/2} f'(\theta)\,\mathrm{d}\theta\right] \tag{25}$$

where

$$f'(\theta) = \left(\frac{W'}{V'}\right)^2 \left(C_N'\cos\theta + C_T'\frac{\sin\theta}{\cos\delta}\right) \tag{26}$$

and $K_0 < 0$ (on the downwind zone).

The upwind nondimensional normal force as a function of the azimuthal angle $\theta$ as a resultant projected in a direction normal to the tower gives a coefficient

$$F_{NX}(\theta) = 2(cH/S)F_{NX}^+ \tag{27}$$

where

$$F_{NX}^+ = \tfrac{1}{2}\int_{-1}^{1}\left(\frac{W}{V_\infty}\right)^2 C_N\,\mathrm{d}\zeta$$

For the upwind half-cycle, the tangential force coefficient is given by the relation

$$F_T(\theta) = 2(cH/S)F_T^{\ddagger} \tag{28}$$

where

$$F_T^{\ddagger} = \tfrac{1}{2}\int_{-1}^{1}\left(\frac{W}{V_\infty}\right)^2\left(\frac{C_T}{\cos\delta}\right)d\zeta$$

Similarly, for the downwind half-cycle of the rotor, we can calculate the normal and tangential force coefficients using Eqs. (27) and (28) where the velocities and blade force coefficients must be replaced by those corresponding to the downwind flow conditions.

The average half-torque coefficients for the upwind and downwind zones are, respectively

$$\bar{C}_Q = \frac{NcH}{2\pi S}\int_{-\pi/2}^{\pi/2}\int_{-1}^{1} C_T\left(\frac{W}{V_\infty}\right)^2\left(\frac{\eta}{\cos\delta}\right)d\zeta\,d\theta \tag{29}$$

$$\bar{C}_Q' = \frac{NcH}{2\pi S}\int_{\pi/2}^{3\pi/2}\int_{-1}^{1} C_T'\left(\frac{W'}{V_\infty}\right)^2\left(\frac{\eta}{\cos\delta}\right)d\zeta\,d\theta \tag{30}$$

The power coefficient for the entire rotor is the weighted sum of the upwind and downwind halves of the rotor.

$$C_p = (\bar{C}_Q + \bar{C}_Q')X_{EQ} \tag{31}$$

## Comparison with Previous Approaches and Test Results

The double-multiple streamtube model with variable interference factors was used to calculate the induced velocities with a modified CARDAAV computer code. The modifications included in the numerical model (CARDAAX) allow the expanding lateral displacement of the streamlines to be determined with respect to an undistorted central streamline. The streamline position, defined by its coordinates, depends on the local tip-speed ratio of the rotor. The upwind and downwind equations are solved separately by an iterative procedure with the airfoil section lift and drag coefficients given by static airfoil data, using both the local Reynolds number and the local angle of attack. Dynamic stall effects are accounted for in the calculations.

To check the significance of the streamtube expansion effects on Darrieus wind turbines a comparison between measured data and previous CARDAAV[13] and VDART code predictions is presented. The test results used for the comparison were obtained from Sandia Laboratories[14,15] for a 5 m machine operating at 162.5 rpm and for a 17 m one at 50.6 rpm. The analytical results were determined by considering the wind shear effect at the Sandia Laboratories test site (a power law profile with an exponent of 10%).

The streamtube width in the undisturbed part of the rotor decreases with the tip-speed ratio (Fig. 2). A similar problem for the Giromill and Darrieus rotor with wake expansion and thus flow retardation in the wake was reported by Wilson,[16] who considered the axial induction factor introduced by Glauert. In Wilson's analysis, the velocity field of the rotor consists of three parts superimposed to obtain the flowfield: freestream velocity and both bound and wake vortex sheets velocities. Comparison between calculated curves of streamlines through the rotor and experiments[10] shows an acceptable physical model for a streamtube expansion (Fig. 3). Figure 4 represents the variation in the angle of attack vs the azimuthal angle for two tip-speed ratios.

The flow divergence between the upwind and downwind regions has been accounted for in the calculation of the downwind induced velocity. The constant interference factor calculated by CARDAA was underestimated in the downwind zone compared with the average of the variable-interference factor (CARDAAV computer code). The CARDAAX code including streamtube expansion effects allows a different variable-interference factor to be calculated but only on the downwind half of the rotor. In this new numerical procedure, the upwind half-cycle of the rotor is assumed to be divided into nine angular tubes corresponding to six angular tubes on the downwind half-cycle zone.

Figure 5 illustrates the contribution of the vertical slices to the power coefficient $C_p$ as a function of the equatorial tip-speed ratio ($X_{EQ} = \omega R/V_\infty$). The Sandia 17 m rotor was divided into 10 vertical slices of equal height and the calculations were made at every azimuthal angle of 5 deg. For each slice the power coefficient was determined with respect to the swept area of the rotor. Each line $X_{EQ} = \text{const}$ represents the power contribution of each slice for a known wind velocity. In this case, at $X_{EQ} = 5.67$ (which corresponds to the total $C_{p\max}$), for example, the contribution of each slice is 35% for the central slice and then 29, 23, 12.5 and 0.5% of $C_p$, respectively (the $C_p$ contribution is given for two symmetrical slices with respect to the equatorial plane). Figure 6 shows the variation in the calculated power coefficient and experimental data for the Sandia 17 m turbine; agreement is good except in the region having tip-speed ratios of 4-6. The numerical data have exhibited a deviation from the experimental data in this region, which represents a transition zone, where all primary effects (or dynamic effects) and secondary effects play a role, albeit on a smaller scale.[12] The difference between two CARDAAX and CARDAAV code calculations (with and without streamtube expansion effects, respectively) is greatest at high tip-speed ratios because it is here that the difference between the induced velocities reaches a maximum. Above a tip-speed ratio of 8, the difference be-

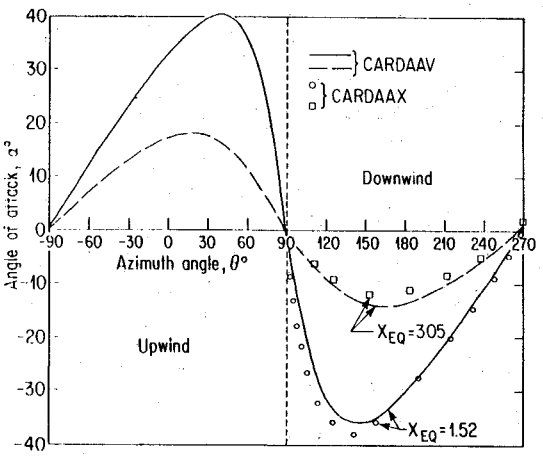


**Fig. 4 Variation of the angle of attack at the equator with the blade position.**

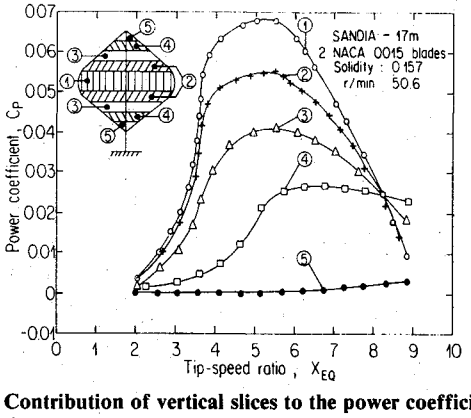


**Fig. 5 Contribution of vertical slices to the power coefficient vs tip-speed ratio.**

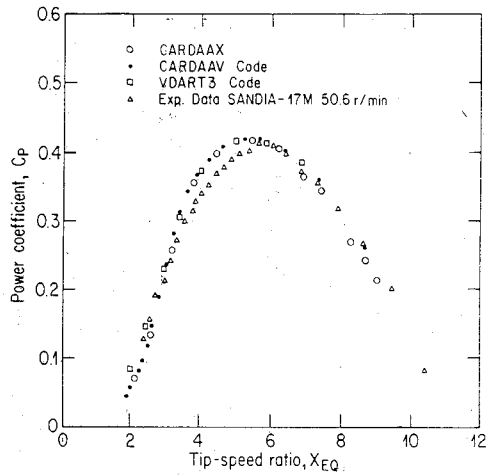


**Fig. 6 Performance comparison between theoretical results and experimental data for the Sandia 17 m turbine.**

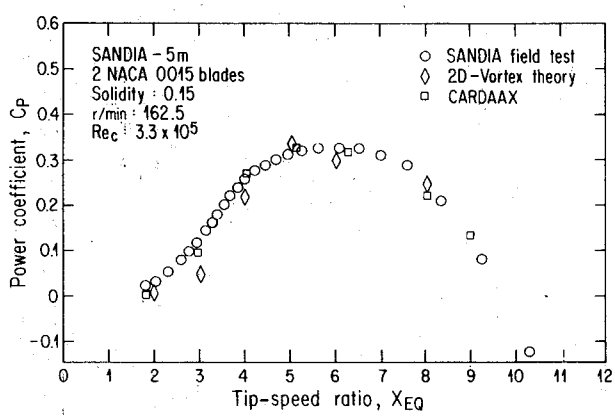


**Fig. 7 Performance comparison between theoretical results and experimental data for the Sandia 5 m turbine.**

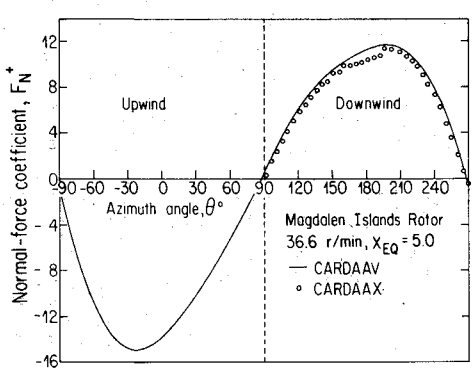


**Fig. 8 Normal-force coefficient as a function of the azimuthal angle.**

tween the power coefficient calculated with the streamtube expansion effect and previous estimations is less than 4%

A comparison of the power coefficients obtained by other models, the present calculations, and the Sandia field test data for two NACA 0015 blades and a 5 m rotor is presented in Fig. 7. Figure 8 illustrates the normal-force coefficient calculated by the CARDAAV and by the CARDAAX computer codes at a tip-speed ratio of $X_{EQ}=5.0$ for the Magdalen Islands rotor (36.6 rpm). The tangential-force coefficient as a function of the azimuthal angle is given in Fig. 9. It can be seen that the streamtube expansion effects result in lower loads compared with previous CARDAAV calculations[12] on the downwind half of the turbine.

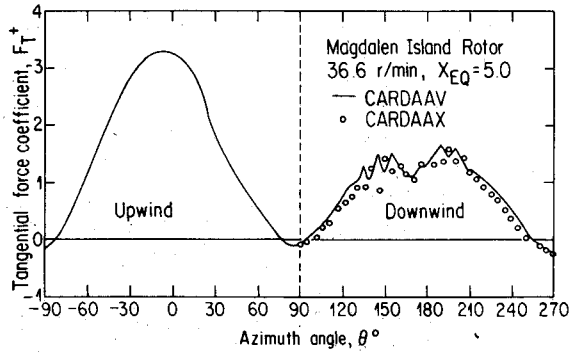


**Fig. 9 Tangential-force coefficient as a function of the azimuthal angle.**

## Conclusions

The proposed modification to the aerodynamic model used to study the Darrieus wind turbine introduces a flow continuity law in the streamtubes through the rotor. Contrary to most authors, it was decided to keep an angular distribution of the calculation points in the downwind part of the rotor in order to maintain the accuracy. The results obtained confirm that this modification yields a second-order improvement in the values obtained previously for low-solidity wind turbines at high tip-speed ratios. The difference in the results is in fact less than 3% for specific tip-speed ratios lower than 6. The streamtube expansion effects result in lower aerodynamic loads, on the downwind part of the rotor, with respect to the previous calculations.

Several studies have demonstrated that the aerodynamic efficiency of Darrieus wind turbines is strongly affected by the blade airfoil geometry. For example, the results given by Ref. 17 show that significant gains in the annual energy output can be achieved with NACA 6-series airfoils. For rotor solidities of 0.07-0.21, Migliore[17] calculated an increase in the annual energy output of 17-27% with a NACA $63_2$-015 compared to a NACA 0015 airfoil. Thus, the airfoil geometry effects are far more significant for VAWT performance than streamtube expansion calculations.

Theoretical and experimental studies are currently under way at Sandia National Laboratories on a second generation of their vertical axis wind turbines. The scope of this work is to develop an optimum Darrieus turbine design[18] using airfoils tailored specifically for vertical axis machines. The new design is supposed to have a large chord width at the ends of the blades and a narrower chord width at the equatorial zone. The blades are divided into many parts of variable length and airfoil cross sections. Thus, a combination of the natural laminar flow airfoils with standard NACA 4-digit airfoils may provide a potentially significant solution reducing the cost of wind energy. The performance characteristics generated by CARDAAX with streamtube expansion effects can be incorporated into the economic model for studying the cost of energy obtained with advanced Darrieus designs.

Further improvements to the model include the possibility of taking account of an observed three-dimensional increase in the tube section and, also, that of defining the distortion of the central line based on the resulting aerodynamic force of the rotor.

## References

[1] Lapin, E. E., "Theoretical Performance of Vertical-Axis Wind Machines," ASME Paper 75-WA/ENER-1, 1975.

[2] Holme, O., "A Contribution to the Aerodynamic Theory of the Vertical-Axis Wind Turbine," Paper presented at International Symposium on Wind Energy Systems, Cambridge, England, Sept. 1976.

[3] Sharpe, D. J. and Read, S., "A Critical Analysis of the Extended Multiple Streamtube Theory for the Aerodynamics of a Vertical Axis Wind Turbine," *Proceedings of the 1982 Wind and Solar Energy*

*Technology Conference,* University of Missouri-Columbia Publications, Kansas City, April 1982, pp. 51-56.

[4]Loth, J. L. and McCoy, H., "Optimzation of Darrieus Turbines with an Upwind and Downwind Momentum Model," *Journal of Energy*, Vol. 7, July-Aug. 1983, p. 313.

[5]Newman, B. G., "Actuator-Disc Theory for Vertical-Axis Wind Turbines," *Journal of Wind Engineering and Industrial Aerodynamics,* Vol. 15, 1983, p. 347.

[6]Paraschivoiu, I., "Aerodynamic Loads and Performance of the Darrieus Rotor," *Journal of Energy,* Vol. 6, Nov.-Dec. 1982, p. 406.

[7]Strickland, J. H., "The Darrieus Turbine: A Performance Prediction Model Using Multiple Streamtubes," Sandia Laboratories, Albuquerque, N. Mex., Rept. SAND75-0431, Oct. 1975.

[8]Templin, R. J., "Double-Multiple Streamtube Theory for Darrieus Rotor Performance Prediction," unpublished notes, March 1981.

[9]Berg, D., "NLF Static Wind Tunnel Test Results, 17-m Torque Measurements, SNL Code Development Summary," Paper presented at Fourth Vertical-Axis Wind Turbine Aerodynamics Seminar, Sandia National Laboratories, Albuquerque, N.M., Jan. 1984.

[10]Comolet, R. and Harajli, I., Mercier des Rochettes, P. and Yeznasni, A., "Sur l'épanouissement du flux á la traversée d'une éolienne Darrieus: théorie et expérience," *C.R.* de l'Académie des Sciences, Paris, Vol. 295, Ser. B, Nov. 1982, pp. 831-834.

[11]Paraschivoiu, I. and Delclaux, F., "Double-Multiple Streamtube Model with Recent Improvements," *Journal of Energy,* Vol. 7, May-June 1983, pp. 250-255.

[12]Paraschivoiu, I., Delclaux, F., Fraunié, P., and Béguier, C., "Aerodynamic Analysis of the Darrieus Rotor Including Secondary Effects," *Journal of Energy,* Vol. 7, Sept.-Oct. 1983, pp. 416-422.

[13]Paraschivoiu, I., "Description des logiciels CARDAA et CARDAAV pour le calcul aérodynamique des éoliennes Darrieus," Institut de Recherche d'Hydro-Québec, Rept. IREQ-8RT3010G, Jan. 1984.

[14]Sheldahl, R. E., Klimas, P. C., and Feltz, L. V., "Aerodynamic Performance of 5-Meter-Diameter Darrieus Turbine with Extruded Aluminum NACA-0015 Blades," Sandia Laboratories, Albuquerque, N. Mex., Rept. SAND 80-0179, March 1980.

[15]Worstell, M. H., "Measured Aerodynamics and Systems Peformance of the 17-m Research Machine," *Proceedings of the Vertical-Axis Wind Turbine Design Technology Seminar for Industry,* edited by S. F. Jhonston, Jr., Albuquerque, N. Mex., April 1980, pp. 233-258.

[16]Wilson, R. E., "Darrieus Rotor Aerodynamics," *Proceedings of the Third Biennial Conference and Workshop on Wind Energy Conversion Systems,* Washington, D. C. Sept. 1977, pp. 584-594.

[17]Migliore, P. G., "Comparison of NACA 6-Series and 4-Digit Airfoils for Darrieus Wind Turbines," *Journal of Energy*, Vol. 7, July-Aug. 1983, pp. 291-292.

[18]Kadlec, E. G., "The Potential of Advanced Darrieus Wind Turbines," *Proceedings of the American Solar Energy Society Annual Meeting, Sixth Biennial Wind Energy Conference,* Minneapolis, Minn., June 1983, pp. 213-218.